

Hydrodynamic fluctuations in a particle-continuum hybrid for complex fluids

Alejandro L. Garcia^{*}, Aleksandar Donev[†], John B. Bell[†] and Berni J. Alder^{**}

^{*}*Department of Physics and Astronomy, San Jose State University, San Jose, California, 95192*

[†]*Center for Computational Science and Engineering, Lawrence Berkeley Nat. Lab., Berkeley, CA, 94720*

^{**}*Lawrence Livermore Nat. Laboratory, P.O.Box 808, Livermore, CA 94551-9900*

Abstract. A previously-developed hybrid particle-continuum method [J. B. Bell, A. Garcia and S. A. Williams, *SIAM Multiscale Modeling and Simulation*, 6:1256-1280, 2008] is generalized to dense fluids and two and three dimensional flows. The scheme couples an explicit fluctuating compressible Navier-Stokes solver with the Isotropic Direct Simulation Monte Carlo (DSMC) particle method [A. Donev and A. L. Garcia and B. J. Alder, *J. Stat. Mech.*, 2009(11):P11008, 2009]. To achieve bidirectional dynamic coupling between the particle (microscale) and continuum (macroscale) regions, the continuum solver provides state-based boundary conditions to the particle subdomain, while the particle solver provides flux-based boundary conditions for the continuum subdomain; see [A. Donev, J.B. Bell, A. Garcia, and B. Alder, *SIAM Multiscale Modeling and Simulation*, 8:871-911, 2010.] for details. This paper summarizes two important numerical tests: First, the equilibrium diffusive (Brownian) motion of a large spherical bead suspended in a particle fluid is examined, demonstrating that the hybrid method correctly reproduces the velocity autocorrelation function of the bead but only if thermal fluctuations are included in the continuum solver. Second, the new scheme is applied to the well-known adiabatic piston problem and we find that it correctly reproduces the slow non-equilibrium relaxation of the piston toward thermodynamic equilibrium but, again, only if the continuum solver includes stochastic (white-noise) flux terms. These two fundamental examples clearly demonstrate the need to include fluctuations in continuum solvers employed in hybrid multiscale methods.

Keywords: Brownian dynamics, Particle/continuum hybrids, Hydrodynamic fluctuations, Multi-scale methods

PACS: 47.11.St, 05.40.Jc

INTRODUCTION

With the increased interest in nano- and micro-fluidics, it has become necessary to develop tools for hydrodynamic calculations at the atomistic scale [1, 2, 3]. While the Navier-Stokes-Fourier continuum equations have been surprisingly successful in modeling microscopic flows [4], there are several effects present at microscopic scales that are difficult to account for in models relying on a purely PDE approximation. For example, it is well known that the Navier-Stokes equations fail to describe flows in the kinetic regions (large Knudsen number flows) that appear in small-scale gas flows [5]. It is also known that hydrodynamic fluctuations play an important role in fluid problems at microscopic and mesoscopic scales, for example in the Brownian motion of suspended microscopic objects. Other examples in which spontaneous fluctuations may significantly affect the dynamics include the breakup of droplets in jets [6, 7, 8], Brownian molecular motors [9], Rayleigh-Bernard convection [10], Kolmogorov flows [11, 12], Rayleigh-Taylor mixing [13], and combustion and explosive detonation [14].

Unfortunately, particle methods, such as DSMC, lack the efficiency necessary to study realistic problems because of the very large numbers of particles needed to fill the required computational domain. Often the computational effort is expended on particles far away from the region of interest, where a description based on the Navier-Stokes equations would be adequate. In this regard hybrid methods are a natural candidate to combine the best features of the particle and continuum descriptions [15, 16]. A particle method can be used in regions where the continuum description fails or is difficult to implement, and a more efficient continuum description can be used around the particle domains.

In a recent paper [17] we describe the implementation of an efficient hybrid for the study of Brownian dynamics. Here we discuss an important result discovered in our testing of this hybrid, namely that the standard, deterministic PDE solver suppresses fluctuations in the particle region, introducing significant errors in the Brownian motion. On the other hand, using a stochastic PDE scheme yields accurate results, as shown in the two cases presented below.

VELOCITY AUTOCORRELATION FUNCTION (VACF) OF A SPHERICAL BEAD

As an illustration of the correct hydrodynamic behavior of the hybrid algorithm, we study the velocity autocorrelation function (VACF) $C(t) = \langle v_x(0)v_x(t) \rangle$ for a large *neutrally-buoyant* impermeable *bead* of mass M and radius R diffusing through a dense Maxwell I-DSMC stochastic fluid [18] of particles with mass $m \ll M$ and collision diameter $D \ll R$ and density (volume fraction) ϕ [mass density $\rho = 6m\phi/(\pi D^3)$]. The VACF problem is relevant to the modeling of polymer chains or (nano)colloids in solution (i.e., *complex fluids*), in particular, the integral of the VACF determines the diffusion coefficient which is an important macroscopic quantity. Furthermore, the very first MD studies of the VACF for fluid molecules led to the discovery of a long power-law tail in $C(t)$ [19] which has since become a standard test for hydrodynamic behavior of methods for complex fluids [20, 21, 22].

The fluctuation-dissipation principle [23] points out that $C(t)$ is exactly the decaying speed of a bead that initially has a unit speed, if only viscous dissipation was present without fluctuations, and the equipartition principle tells us that $C(0) = \langle v_x^2 \rangle = kT/2M$. Using these two observations and assuming that the dissipation is well-described by a continuum approximation with stick boundary conditions on a sphere of radius R_H , $C(t)$ has been calculated from the linearized (compressible) Navier-Stokes (NS) equations [24, 25]. The results are analytically complex even in the Laplace domain, however, at short times an inviscid compressible approximation applies. At large times the compressibility does not play a role and the incompressible NS equations can be used to predict the long-time tail [25, 26]. At short times, $t < t_c = 2R_H/c_s$, the major effect of compressibility is that sound waves generated by the motion of the suspended particle carry away a fraction of the momentum with the sound speed c_s , so that the VACF quickly decays from its initial value $C(0) = k_B T/M$ to $C(t_c) \approx k_B T/M_{eff}$, where $M_{eff} = M + 2\pi R^3 \rho/3$ [25]. At long times, $t > t_{visc} = 4\rho R_H^2/3\eta$, the VACF decays as with an asymptotic power-law tail $(k_B T/M)(8\sqrt{3}\pi)^{-1}(t/t_{visc})^{-3/2}$, in disagreement with predictions based on the Langevin equation (Brownian dynamics), $C(t) = (k_B T/M)\exp(-6\pi R_H \eta t/M)$.

We performed purely particle simulations of a diffusing bead in various I-DSMC fluids in Refs. [18, 22]. In purely particle methods the length of the runs necessary to achieve sufficient accuracy in the region of the hydrodynamic tail is often prohibitively large for beads much larger than the fluid particles themselves. It is necessary to use hybrid methods and limit the particle region to the vicinity of the bead in order to achieve a sufficient separation of the molecular, sonic, viscous, and diffusive time scales and study sufficiently large box sizes over sufficiently long times. The interaction between the I-DSMC fluid particles and the bead is treated as if the fluid particles are hard spheres of diameter D_s , chosen to be somewhat smaller than their interaction diameter with other fluid particles (specifically, we use $D_s = D/4$) for computational efficiency reasons, using an event-driven algorithm [27]. Upon collision with the bead the relative velocity of the fluid particle is reversed in order to provide a no-slip condition at the surface of the suspended sphere [27] (slip boundaries give qualitatively identical results). We have estimated the effective (hydrodynamic) colloid radius R_H from numerical measurements of the Stokes friction force $F = -6\pi R_H \eta v$ and found it to be somewhat larger than the hard-core collision radius $R + D_s/2$, but for the calculations below we use $R_H = R + D_s/2$.

For the hybrid calculations, we localize the particle subdomain to the continuum cells that overlap or are close to the moving bead. The location of the particle subdomain is updated periodically as the bead moves. The algorithm that we use tries to fit the particle subdomain as closely around the bead while ensuring that there are a certain number of micro cells in-between the surface of the bead and the particle-continuum interface. The exact shape of the particle subdomain thus changes as the bead moves and the number of particles employed by the hybrid fluctuates, especially when the bead is small compared to the continuum cells. In the calculations shown in Fig. 1, the I-DSMC fluid has a density (volume fraction) $\phi = 0.5$ and collision frequency prefactor $\chi = 0.62$. The adiabatic sound speed is $c_s = \sqrt{5k_B T/(3m)}$ and viscosity is $\eta = \tilde{\eta} D^{-2} \sqrt{mk_B T}$, where we measured $\tilde{\eta} \approx 0.75$. Note that in atomistic time units $t_0 = D\sqrt{m/k_B T}$ the viscous time scale is $t_{visc}/t_0 \approx 6\phi(R_H/D)^2/(3\pi\tilde{\eta}) \approx 0.4(R_H/D)^2$.

As a first test case, in Fig. 1 (left) we compare against the particle data from Ref. [22], for which the size of the bead is $R = 1.25D$, $M = 7.81m$, and the simulation box is $L = 1 = 25D$, which corresponds to 24^3 micro cells and about $N \approx 1.5 \cdot 10^4$ particles. The hybrid runs used macro cells each composed of 4^3 micro cells, which corresponds to about $N_0 = 80$ particles per cell, and the size of the particle subdomain fluctuated between about $3 \cdot 10^3$ and $6 \cdot 10^3$ particles due to the change of the location of the bead relative to the continuum grid. The particle result is the average over 10 runs, each of length $t/t_{visc} \approx 2 \cdot 10^5$, while the hybrid results are from a single run of length $t/t_{visc} \approx 7.5 \cdot 10^5$. It is seen in the figure that both the deterministic and the fluctuating hybrid reproduce the particle results closely, with a small but visible difference at long times where the deterministic hybrid under-predicts the magnitude of the tail in the VACF. We also show results from a hybrid run with a twice larger simulation box, $L = 2$, which marginally increases the computational effort in the hybrid runs, but would increase the length of purely particle runs by an order of magnitude.

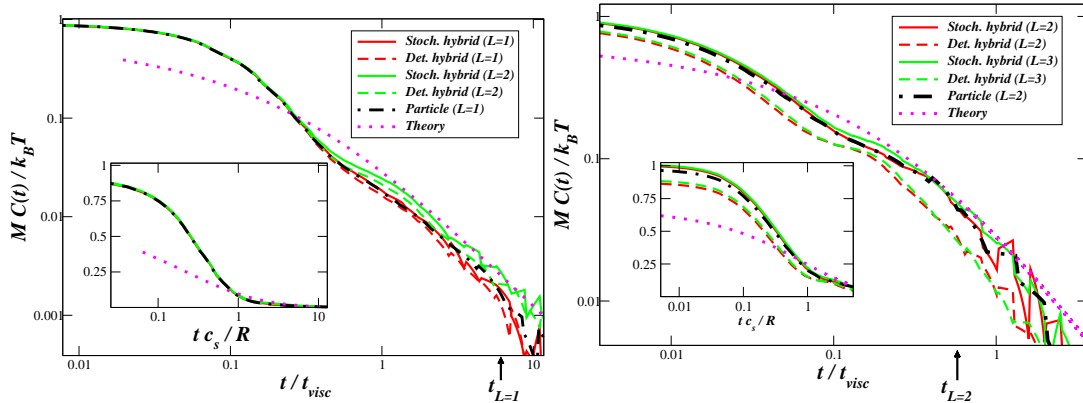


FIGURE 1. Normalized velocity autocorrelation function (VACF) $C(t)/(k_B T/M)$ for a neutrally-buoyant hard spherical bead of mass M suspended in a fluid of I-DSMC particles of diameter D , for two different bead sizes, a small bead of radius $R = 1.25D$ (left) and a large bead of radius $R = 6.25D$ (right). A log-log scale is used to emphasize the long-time power law tail and the time is normalized by the viscous time t_{visc} , so that the results should be approximately independent of the actual bead radius. The inset shows the initial decay of the VACF on a semi-log scale, where the time is normalized by the sonic time scale t_c . Periodic boundary conditions with a cubic cell of length L are employed, and the sound crossing time t_L is indicated. Results from purely particle simulations are shown with a dashed-dotted line, and the incompressible hydrodynamic theory is shown in with a dotted line. Results from hybrid runs are also shown with a solid line for the stochastic hybrid and dashed line for the deterministic hybrid, for both the same box size as the particle runs (red) and a larger simulation box (green).

The hydrodynamic tail becomes pronounced and closer to the theoretical prediction for an infinite system, as expected.

As a second, more difficult test, in Fig. 1 (right) we report results from particle simulations for a much larger bead, $R = 6.25D$, $M = 976m$, and the simulation box is $L = 2 = 50D$, which corresponds to $N \approx 1.2 \cdot 10^5$ particles. We have performed a variety of hybrid runs and Fig. 1 (right) shows results from runs with macro cells each 3^3 micro cells, as well as results for a larger simulation box, $L = 3$, and macro cells each composed of 4^3 micro cells. The particle results are the average over 5 runs each of length $t/t_{\text{visc}} \approx 2.5 \cdot 10^3$, while the hybrid results are from a single run of length $t/t_{\text{visc}} \approx 7.5 \cdot 10^3$. The hybrid runs had a particle subdomain containing about $2 \cdot 10^4$ particles. We observed little impact of the size of the continuum cell size or the size of the particle subdomain. The results show that the stochastic hybrid correctly reproduces the tail in the VACF, while it slightly over-estimates the VACF at short times. The deterministic hybrid, on the other hand, strongly under-estimates the magnitude of $C(t)$ at both short and long times. It is particularly striking that the deterministic hybrid fails to reproduce the magnitude of the long time tail (and thus the diffusion coefficient), demonstrating the importance of including fluctuations in the continuum domain.

RELAXATION OF AN ADIABATIC PISTON

The problem of how thermodynamic equilibrium is established has a long history in statistical mechanics [28]. The *adiabatic piston problem* is one of the examples used to study the fluctuation-driven relaxation toward equilibrium [29, 30, 31] that is simple enough to be amenable to theoretical analysis but also sufficiently realistic to be relevant to important problems in nano-science such as Brownian motors [9, 32]. We study the following formulation of the adiabatic piston problem. A long quasi one-dimensional box with adiabatic walls is divided in two halves with a thermally-insulating piston of mass $M \gg m$ that can move along the length of the box without friction. Each of the two halves of the box is filled with a fluid that is, initially, at a different temperature T and density ρ , here assumed to follow the ideal equation of state $P = \rho k_B T/m$. If the macroscopic pressures in the two halves are different, $\rho_L T_L \neq \rho_R T_R$, then the pressure difference will push the piston to perform macroscopic oscillations with a period that can be estimated by assuming that each half undergoes an adiabatic transformation ($PV^\gamma = \text{const.}$). These oscillations are damped by viscous friction and lead to the piston essentially coming to rest in a state of *mechanical equilibrium*, $\rho_L T_L = \rho_R T_R$. This stage of the relaxation from non-equilibrium to mechanical equilibrium has been shown to be well-described by deterministic hydrodynamics [30].

The state of mechanical equilibrium is however not a state of true thermodynamic equilibrium, which also requires equality of the temperatures on the two sides of the piston. Reaching full equilibrium requires heat transfer through the

piston, but the piston is adiabatic and does not conduct heat. In classical deterministic hydrodynamics the piston would just stand still and never reach full equilibrium. It has been realized long ago that heat is slowly transferred through the mechanical asymmetric fluctuations of the piston due to its thermal motion, until the temperatures on both sides of the piston equilibrate and the fluctuations become symmetric. This equilibration takes place through a single degree of freedom (the piston position) coupling the two large reservoirs, and it would be astronomically slow in a macroscopic laboratory setting. While various Langevin or kinetic theories have been developed for the effective heat conduction of the adiabatic piston (see Refs. [29, 30, 31] and references therein), there is no complete theoretical understanding of the effective heat conductivity, especially in dense fluids. Molecular dynamic simulations have been performed in the past [29, 30] using hard-disk fluids, but the very long runs required to reach thermodynamic equilibrium for massive pistons have limited the size of the systems that could be studied.

Here we apply our hybrid method to the adiabatic piston problem in two dimensions, using a non-linear two-dimensional implementation of the Runge-Kutta integrator described in Ref. [33] as the continuum solver. The choice of two dimensions is for purely computational reasons. Firstly, the number of particles required to fill a box of sufficient size is much smaller thus allowing for long particle simulations. Secondly, in order to implement the piston in our particle scheme we reused the same mixed event-driven/time-driven handling [27] as we used for the VACF computations. Namely, we made a piston out of N_b small impermeable beads, connected together to form a barrier between the two box halves, as illustrated in Fig. 2. In two dimensions, by ensuring that two piston beads never separate by more than a given distance we can ensure that two I-DSMC particles on opposite sides of the piston cannot possibly collide and thus the piston will be insulating. We have studied two different types of pistons, a *flexible* piston where the beads are tethered together to form a chain [27] that is stretched but where each individual bead can still move independently of the others, and a *rigid* piston that is obtained with a slight modification of the event loop to move all of the piston beads in unison. While at the macroscopic level the exact shape of the piston should not make a big difference, we have found that increasing the number of degrees of freedom of the piston from one to N_b makes a significant difference in the thermal conductivity of the piston, and therefore, we will focus here on rigid pistons as in the traditional formulation.

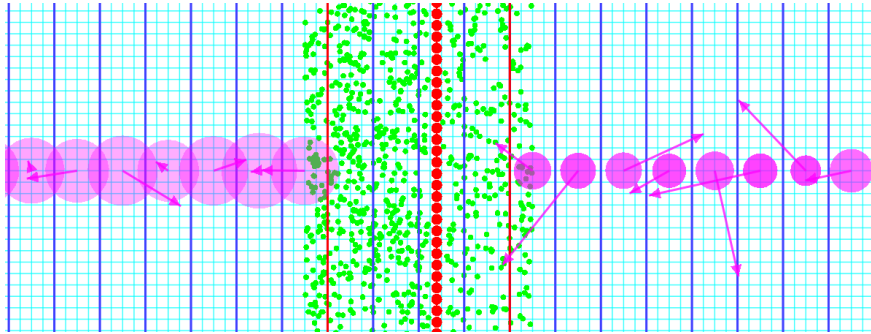


FIGURE 2. An illustration of the computational setup used for the adiabatic piston computations. Only the central portion of the box of aspect ratio 6×1 is shown. Left of the piston the gas is cold and dense; to the right it is hot and dilute. The piston beads (red disks) separate the box into two halves, and are surrounded on each side by a fluid of I-DSMC particles (smaller green disks), which is twice denser but also twice cooler in the left half than in the right half. The microscopic grid is shown with thinner light blue lines and the hydrodynamic grid is shown with thicker dark blue lines. The interface between the particle and continuum regions is highlighted with a thick red line. A snapshot of the values of the hydrodynamic variables in each continuum cell is shown using a large purple disk whose size is proportional to the density and its opacity is proportional to the temperature, and an arrow for the fluctuating velocities.

The hybrid method setup for the adiabatic piston is illustrated in Fig. 2. We use a two-dimensional Maxwell I-DSMC particle fluid ($\phi = 1$, $\chi = 1$) with collision diameter $D = 0.1$ (hard-sphere diameter $D_s = D/2$) and a piston composed of $N_b = 40$ beads of diameter $D_b = 0.0955$. The particle subdomain is limited to a few continuum cells around the piston, which we keep at about two or more continuum cells on each side of the piston, so that the unreasonable hydrodynamic values in the cells that overlap the piston do not affect the continuum solver appreciably. Periodic boundary conditions are applied along the y dimension (parallel to the piston) with the width of the domain $L_y = 4$ being 40 microscopic cells, while adiabatic walls were placed at the ends of the box whose total length $L_x = 24$ was 240 microscopic cells. We have studied various sizes for the macroscopic cells, and report results for a quasi one-dimensional continuum grid in which each macro cell contains 4×40 micro cells, corresponding to about 200 particles per continuum cell. We also present results for a two-dimensional continuum grid where each macro cell contains 8×10 micro cells.

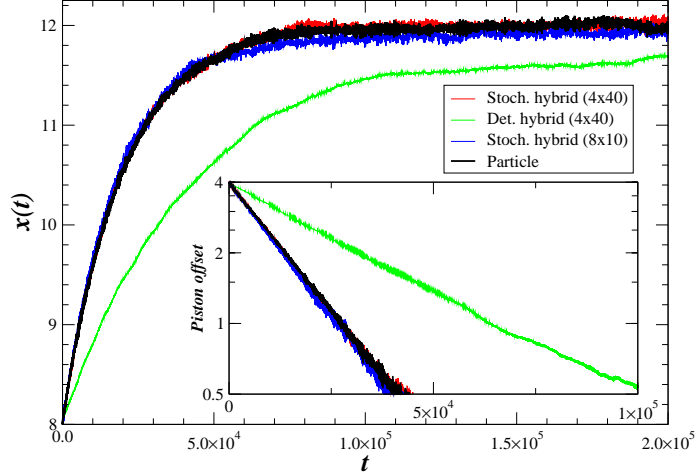


FIGURE 3. Relaxation of a rigid piston of mass $M/m = 1000$ from an initial state of mechanical equilibrium ($x = 8$) to a state of thermodynamic equilibrium ($x = 12$). The inset emphasizes the initial exponential decay on a semi-log scale. The hybrid runs used a particle subdomain of width $w_p = 2$ on each side of the piston and continuum cells that were composed of either 4×40 or 8×10 microscopic cells. For the deterministic hybrid the macro cell size makes little difference so we only show the 4×40 case.

A comparison of the all-particle, stochastic-PDE hybrid, and deterministic-PDE hybrid results is shown in Fig. 3 for the relaxation of a piston of mass $M = 1000m$ initially in mechanical equilibrium at position $x = 8 = L_x/3$. The initial conditions were $k_B T_L = 2/3$, $\rho_L = 2/3$ and $k_B T_R = 4/3$, $\rho_R = 1/3$, so that there is an equal mass on each side of the piston. At the true equilibrium state the piston remains close to the middle of the box, $x_{eq} = L/2 = 12$, with equal density on each side. The results shown are averages over 10 samples, but it should be emphasized that each run exhibits thermal oscillations of the piston position that are diminished by direct averaging because they have different (random) phases. At thermodynamic equilibrium, the frequency of thermally-driven oscillations, estimated using a quasi-adiabatic harmonic approximation, is $\omega^2 \approx Nk_B T / [Mx(L_x - x)]$ and the amplitude of the oscillations is on the order of $\Delta x^2 \approx x(L_x - x)/N$, where N is the number of particles per chamber. Figure 3 shows that the stochastic hybrid is able to correctly reproduce the rate of exponential relaxation of the piston toward equilibrium with many fewer particles than the purely particle runs, while the deterministic hybrid fails. We find a slight dependence on the exact details of the hybrid calculations such as cell size or the width of the particle subdomain, however, in general, the stochastic hybrid is remarkably robust and accurate. At the same time, the importance of including thermal fluctuations in the continuum subdomain is evident, just as we observed for the VACF computations in the previous section.

SUMMARY AND CONCLUSIONS

This paper presents two cases in which hybrid particle/continuum calculations were performed to study systems with Brownian motion. Our results for both the neutrally-buoyant bead and the adiabatic piston clearly demonstrate that a large massive suspended body cannot have the correct Brownian dynamics unless thermal fluctuations are consistently included in the *full* computational domain. Massive and large suspended bodies have longer relaxation times and thus it is not surprising that long-wavelength, slowly-decaying, hydrodynamic fluctuations play a prominent role. Although we earlier reported [34, 35, 36, 37] a suppression of fluctuations in the particle region of a hybrid using a continuum PDE solver, the impact on the Brownian dynamics is surprisingly significant. Thus for multi-scale problems of this type in the continuum region of particle/continuum hybrid one must use a stochastic hydrodynamic scheme, such as those described in [33], even if a large particle subdomain is used.

REFERENCES

1. H. Noguchi, N. Kikuchi, and G. Gompper. Particle-based mesoscale hydrodynamic techniques. *Europhysics Letters*, 78:10005, 2007.

2. R. Delgado-Buscalioni, K. Kremer, and M. Praprotnik. Concurrent triple-scale simulation of molecular liquids. *J. Chem. Phys.*, 128:114110, 2008.
3. G. Hu and D. Li. Multiscale phenomena in microfluidics and nanofluidics. *Chem. Eng. Sci.*, 62(13):3443–3454, 2007.
4. T. M. Squires and S. R. Quake. Microfluidics: Fluid physics at the nanoliter scale. *Rev. Mod. Phys.*, 77(3):977, 2005.
5. N. G. Hadjiconstantinou. The limits of Navier-Stokes theory and kinetic extensions for describing small-scale gaseous hydrodynamics. *Physics of Fluids*, 18(11):111301, 2006.
6. M. P. Brenner, X. D. Shi, and S. R. Nagel. Iterated instabilities during droplet fission. *Phys. Rev. Lett.*, 73(25):3391–3394, 1994.
7. M. Moseler and U. Landman. Formation, stability, and breakup of nanojets. *Science*, 289(5482):1165–1169, 2000.
8. J. Eggers. Dynamics of liquid nanojets. *Phys. Rev. Lett.*, 89(8):084502, 2002.
9. C. Van den Broeck, P. Meurs, and R. Kawai. From Maxwell demon to Brownian motor. *New Journal of Physics*, 7:10, 2005.
10. M. Wu, G. Ahlers, and D.S. Cannell. Thermally induced fluctuations below the onset of Rayleigh-Bénard convection. *Phys. Rev. Lett.*, 75(9):1743–1746, 1995.
11. I. Bena, M. Malek Mansour, and F. Baras. Hydrodynamic fluctuations in the Kolmogorov flow: Linear regime. *Phys. Rev. E*, 59(5):5503–5510, 1999.
12. I. Bena, F. Baras, and M. Malek Mansour. Hydrodynamic fluctuations in the Kolmogorov flow: Nonlinear regime. *Phys. Rev. E*, 62(5):6560–6570, 2000.
13. K. Kadau, C. Rosenblatt, J. L. Barber, T. C. Germann, Z. Huang, P. Carles, and B. J. Alder. The importance of fluctuations in fluid mixing. *PNAS*, 104(19):7741–7745, 2007.
14. A. Lemarchand and B. Nowakowski. Fluctuation-induced and nonequilibrium-induced bifurcations in a thermochemical system. *Molecular Simulation*, 30(11-12):773–780, 2004.
15. H. S. Wijesinghe and N. G. Hadjiconstantinou. Discussion of hybrid atomistic-continuum methods for multiscale hydrodynamics. *International Journal for Multiscale Computational Engineering*, 2(2):189–202, 2004.
16. K. M. Mohamed and A. A. Mohamad. A review of the development of hybrid atomistic-continuum methods for dense fluids. *Microfluidics and Nanofluidics*, pages 1–20, 2009.
17. A. Donev, J.B. Bell, A. Garcia, and B. Alder. A hybrid particle-continuum method for hydrodynamics of complex fluids. *SIAM Multiscale Modeling and Simulation* 8:871-911, 2010.
18. A. Donev, A. L. Garcia, and B. J. Alder. A Thermodynamically-Consistent Non-Ideal Stochastic Hard-Sphere Fluid. *Journal of Statistical Mechanics: Theory and Experiment*, 2009(11):P11008, 2009.
19. B. J. Alder and T. E. Wainwright. Decay of the velocity autocorrelation function. *Phys. Rev. A*, 1(1):18–21, 1970.
20. N. Sharma and N. A. Patankar. Direct numerical simulation of the Brownian motion of particles by using fluctuating hydrodynamic equations. *J. Comput. Phys.*, 201:466–486, 2004.
21. P. J. Atzberger. Velocity correlations of a thermally fluctuating Brownian particle: A novel model of the hydrodynamic coupling. *Physics Letters A*, 351(4-5):225–230, 2006.
22. A. Donev, A. L. Garcia, and B. J. Alder. Stochastic Hard-Sphere Dynamics for Hydrodynamics of Non-Ideal Fluids. *Phys. Rev. Lett.*, 101:075902, 2008.
23. R. Kubo. The fluctuation-dissipation theorem. *Reports on Progress in Physics*, 29(1):255–284, 1966.
24. E. H. Hauge and A. Martin-Lof. Fluctuating hydrodynamics and Brownian motion. *J. Stat. Phys.*, 7(3):259–281, 1973.
25. R. Zwanzig and M. Bixon. Compressibility effects in the hydrodynamic theory of Brownian motion. *J. Fluid Mech.*, 69:21–25, 1975.
26. T. V. Lokotosh and N. P. Malomuzh. Lagrange theory of thermal hydrodynamic fluctuations and collective diffusion in liquids. *Physica A*, 286(3-4):474–488, 2000.
27. A. Donev, A. L. Garcia, and B. J. Alder. Stochastic Event-Driven Molecular Dynamics. *J. Comp. Phys.*, 227(4):2644–2665, 2008.
28. E. Lieb. Some problems in statistical mechanics that I would like to see solved. *Physica A*, 263(1-4):491–499, 1999.
29. E. Kestemont, C. Van den Broeck, and M. Malek Mansour. The 'adiabatic' piston: And yet it moves. *Europhysics Letters (EPL)*, 49(2):143–149, 2000.
30. M. Malek Mansour, A. L. Garcia, and F. Baras. Hydrodynamic description of the adiabatic piston. *Phys. Rev. E*, 73(1):016121, 2006.
31. M. Cencini, L. Palatella, S. Pigolotti, and A. Vulpiani. Macroscopic equations for the adiabatic piston. *Phys. Rev. E*, 76(5):051103, 2007.
32. C. Bustamante, J. Liphardt, and F. Ritort. The nonequilibrium thermodynamics of small systems. *Physics Today*, 58(7):43–48, 2005.
33. A. Donev, E. Vanden-Eijnden, A. L. Garcia, and J. B. Bell. On the Accuracy of Explicit Finite-Volume Schemes for Fluctuating Hydrodynamics. *Communications in Applied Mathematics and Computational Science*, 5:149–197, 2010.
34. F. Alexander, A. L. Garcia, and D. Tartakovsky. Algorithm Refinement for Stochastic Partial Differential Equations: I. Linear Diffusion. *J. Comp. Phys.*, 182:47–66, 2002.
35. F. Alexander, A. L. Garcia, and D. Tartakovsky. Algorithm Refinement for Stochastic Partial Differential Equations: II. Correlated Systems. *J. Comp. Phys.*, 207:769–787, 2005.
36. J. B. Bell, J. Foo, and A. L. Garcia. Algorithm refinement for the stochastic Burgers equation. *J. Comp. Phys.*, 223(1):451–468, 2007.
37. S. A. Williams, J. B. Bell, and A. L. Garcia. Algorithm Refinement for Fluctuating Hydrodynamics. *SIAM Multiscale Modeling and Simulation*, 6:1256–1280, 2008.